Title
4 DATA OF RELATIVISTIC NUCLEAR COLLISIONS

Author
Gutbrod, H.H.

Publication Date
1983-05-01

Lawrence Berkeley Laboratory
UNIVERSITY OF CALIFORNIA

Presented at the International Topical Meeting on
High Energy Nuclear Physics, Balatonfüred.
Hungary, June 6-11, 1983

4π DATA OF RELATIVISTIC NUCLEAR COLLISIONS

H.H. Gutbrod, H.A. Gustafsson, B. Kolb, H. Löhner,
B. Ludewigt, A.M. Poskanzer, T. Renner, H. Riedesel,
H.G. Ritter, A. Warwick, F. Weik, and H. Wieman

May 1983

NUCLEAR SCIENCE DIVISION

Prepared for the U.S. Department of Energy under Contract DE-AC03-76SF00098

DISCLAIMER

LBL-16110

4π data of relativistic nuclear collisions

H.H. Gutbrod, H.A. Gustafsson, B. Kolb, H. Löhner,
B. Ludewigt, A.M. Poskanzer, T. Renner, H. Riedesel,
H.G. Ritter, A. Warwick, F. Weik, and H. Wieman

Gesellschaft für Schwerionenforschung, Planckstrasse 1
D-6300 Darmstadt 11, West Germany
and
Nuclear Science Division, Lawrence Berkeley Laboratory
University of California, Berkeley, CA 94720

International Topical Meeting on "High Energy Nuclear Physics"
Sixth International Balaton Topical Conference
Balatonfüred, Hungary, June 6-11, 1983

This work was supported in part by the Director, Office of Energy Research, Division of Nuclear Physics of the Office of High Energy and Nuclear Physics of the U.S. Department of Energy under Contract DE-AC03-76SF00098.

4π data of relativistic nuclear collisions

H.H. Gutbrod, H.A. Gustafsson, B. Kolb, H. Löhner,
B. Ludewigt, A.M. Poskanzer, T. Renner, H. Riedesel,
H.G. Ritter, A. Warwick, F. Weik, H. Wieman

Gesellschaft für Schwerionenforschung, Planckstrasse 1
D-6300 Darmstadt 11, West Germany and
Nuclear Science Division, Lawrence Berkeley Laboratory
University of California, Berkeley, CA 94720, USA

During the past two years, complete events of relativistic nuclear collisions are being studied with the Plastic Ball, the first electronic nonmagnetic particle-identifying 4π spectrometer[1]. It is well suited to handle the large multiplicities in these reactions and allows collection of data at a rate sufficient to make further software selections to look at rare events.

The analysis of the data follows various lines covering topics like thermalization, stopping or transparency, cluster-production mechanism (--can it tell entropy?), search for collective flow through various global analyzing methods that allow determination of the scattering plane, projectile fragmentation (--is there a bounce-off?), pion distribution, two-particle correlations: Hanbury-Brown Twiss, and excited nuclear states (--nucleosynthesis at the freezeout point or from chemical equilibrium?). We will cover in this contribution only two subjects: "stopping and thermalization" and "cluster production".

Stopping and Thermalization in Relativistic Nuclear Heavy Ion Collisions

One of the major hopes of relativistic nuclear heavy ion physics is to study the equation of state of nuclear matter at large densities. For that it is of utmost importance to find experimentally a signature that justifies the concept of matter properties like density, temperature, chemical equilibrium, etc.

The aspect of full thermalization among the participant nucleons has been postulated in the early nuclear fireball model[2], which in a later version included also chemical equilibrium for pions, nucleons, and composite particles[3,4]. Discrepancies with data[5] lead to the discussion, e.g., of the validity of hydrodynamics, the transparency of nuclei, and the mean free path of nucleons in these "dense" reaction zones.

Because thermalization is the randomizing of the longitudinal energy over all degrees of freedom, one can look in each event for the momentum distribution of the fragments in the cm system (for equal mass target and projectile combinations the center of mass is identical with the nucleon-nucleon center of mass, ignoring fluctuations). For an isotropically expanding system with N particles, one finds in the center-of-mass frame from simple phase space considerations[6]

$$\frac{1}{2} \sum_i p_{i\perp}^2 = \sum_i p_{i\parallel}^2 \qquad \text{(equal partition theorem)}$$

or (1)

$$R = \frac{2}{\pi} \frac{\sum |p_{i\perp}|}{\sum |p_{i\parallel}|} = 1$$

A global stopping of the two nuclei at small impact parameters would show up in a ratio R = 1 or even larger if hydrodynamical flow into transverse direction exists. In the presence of transparency this ratio would always be below 1. Data that fulfill the necessary condition of eq. (1) can be said to indicate a nuclear fireball if, in addition, their energy spectra are of Maxwell Boltzmann shape in the center of mass.

Complete events have been measured with the Plastic Ball, a particle-identifying 4π spectrometer[1] for Ca + Ca and Nb + Nb at E/A = 400. Beside a minimum biased reaction trigger data were taken requiring the absence of particles with projectile velocity in a forward cone of $\theta_{lab} = \pm 2$. This trigger enriched the sample of high multiplicity events that dominantly originate from more central collisions.

In fig. 1 (top) contour lines of the yield of events in the plane $2/\pi \ \Sigma |p_{i\perp}|/A$ vs $\Sigma |p_{i\parallel}|/A$ are shown for the system Ca + Ca, the minimum bias trigger applied. Most of the yield is far away from the R = 1 region. The peak at small $p_\perp$ but large $p_\parallel$ corresponds to peripheral reactions and is dominated by projectile fragments. This contribution vanishes as the trigger is changed to a "central" one. Figure 1 (middle) shows central trigger events with a charge particle multiplicity larger than 30. The maximum of the yield is shifted toward the diagonal but only a few events reach R = 1, which, for large multiplicities and absence of any two jet structure, corresponds to a full stopping of the nuclei. In the lower part of fig. 1 for the reaction of 400 MeV/u Nb + Nb the central trigger events with charge particle multiplicities beyond 55 are fulfilling the stopping condition (R = 1 ±0.05) on the average.

The observed difference between the Ca + Ca and the heavier Nb + Nb system allows different interpretations: a) The Ca nuclei are too small to stop one another, so a transparency remains in the longitudinal direction. b) Only a subvolume is fully stopped and eventually thermalized, but the surface zones show some transparency and therefore the differences are caused by the various surface-to-volume ratios of Ca and Nb.

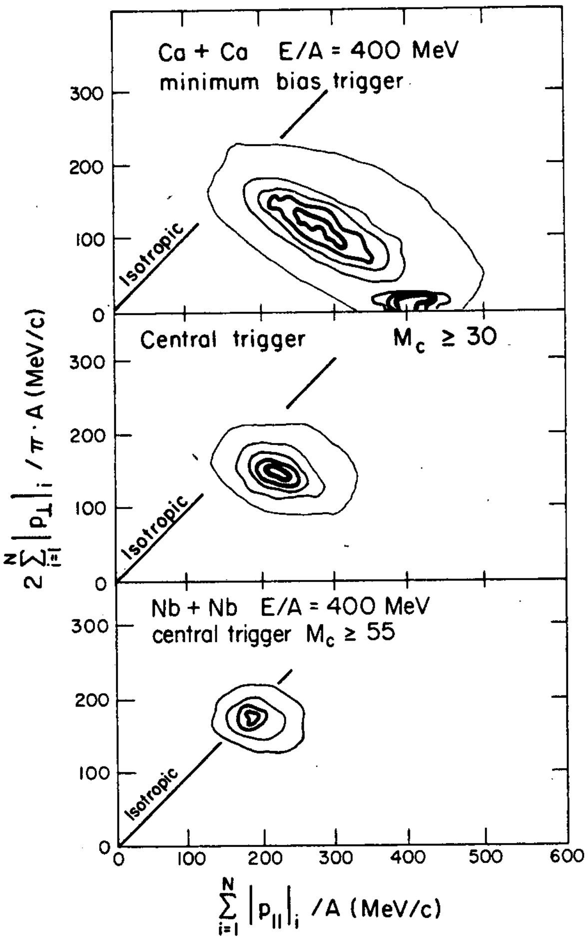

Fig. 1

However, one has to keep in mind that the high multiplicity cuts correspond roughly to an impact parameter selection from 0 to 3 fm, where in these symmetric systems still large parts of the nuclei might pass one another rather undisturbed. Although spectator fragments are excluded within $\theta_{lab} \le 2^\circ$ with our central trigger condition, there are still some "leading particles" left outside of $\theta_{lab} = 2^\circ$. Any one of these particles strongly enhances the parallel momentum component, thus reducing the ratio R.

Since both explanations—surface and transparency—are subject to these spectator contributions, it is useful to study the perpendicular momentum transfer in the reaction at the highest multiplicities. This has been done by analyzing proton spectra at $\theta_{cm} = 90^\circ$ with a relativistic Maxwell Boltzmann distribution with σ_0 and T_0 as free parameters.

$$\frac{d\sigma}{p^2 dp\, d\Omega} = \frac{\sigma_0}{4\pi m^3} \frac{e^{-E/T_0}}{K(m/T_0)} \quad (2)$$

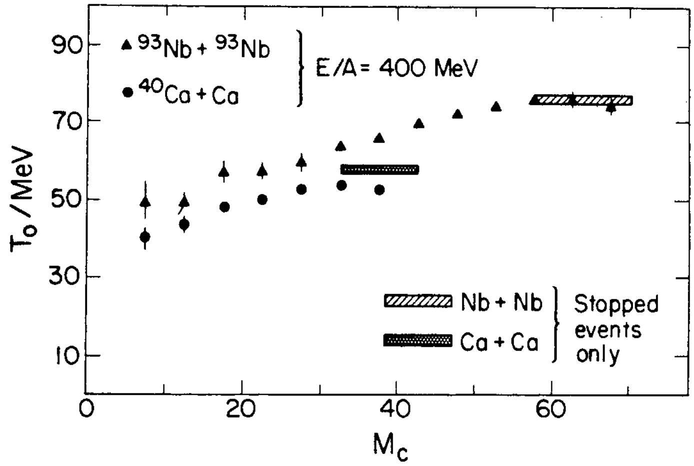

Fig. 2

Figure 2 shows T_0 values extracted from proton spectra at $\theta_{cm} = 90^\circ$ as a function of the charged particle multiplicity M_c. One observes an increase in T_0 with increasing multiplicity for both systems measured, but at comparable multiplicities the Nb data lie above those of Ca. For events where the stopping criterion (eq. (1)) is fulfilled T_0 values have been extracted and are indicated by the shaded areas. Their 90° proton spectra are presented in fig. 3a and the extracted slope parameter T_0 = 76 MeV for Nb + Nb and T_0 = 58 MeV for Ca + Ca can be called the temperatures of these fireballs.

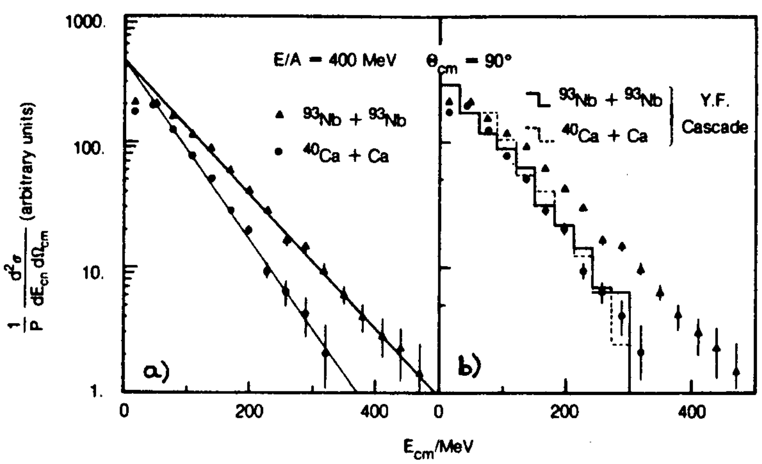

Fig. 3

Taking these temperatures and assuming a source moving with cm velocity in beam direction the energy spectra in the laboratory system between $\theta_{lab} = 20^\circ$ and 160° are well described, slightly better for Nb than for Ca. The standard fireball model[3], size independent, predicts a temperature of 60–70 MeV. The temperature is lowered by the pion production and increased by composite particle production by several MeV through the decrease of degrees of freedom.

The d/p ratios of the highest multiplicity events, M_c = 35 for Ca + Ca and M_c = 55 for Nb + Nb, are only 20% larger for the heavier system and therefore can partially cause the observed temperature difference[8]. However, the difference in slope parameters T_0 at the same multiplicity as well as the higher than fireball temperature for Nb can not be explained simply.

The histograms in fig. 3b are intranuclear cascade calculations[7] for the two systems. The INC model clearly underestimates the yield for Nb at large $p_\perp$. It seems therefore necessary to include nucleon-cluster collisions, as suggested by Remler[9], which allow the nucleon to scatter to larger angles. Similar to the nuclear fireball with chemical equilibrium such a model will produce more yield at large $p_\perp$ contrary to a pure final state coalescence model, which dominantly reduces the low momentum proton yield for composite particle production.

Composite Particle and Entropy Production

Models of relativistic nuclear collisions that include the equation of state of nuclear matter predict an increase in entropy for a phase transition at high nuclear density[10]. Recently it was pointed out[11] that entropy can be related to cluster production, in particular to the ratio of deuteron yield to proton yield. This has stimulated a dispute among theorists over whether the information about the early state inherent in this ratio gets lost during the expansion phase or is disturbed only via second order effects, whether the deuteron and proton yields are the proper observables, or whether one should use the quantities deuteron-like and proton-like defined[12] as d-like = d + 1.5 (^{3}He + ^{3}H) + 3 ^{4}He and p-like = p + d + t + 2 (^{3}He + ^{4}He). Until now these studies have been limited to single particle inclusive data, which mix together reactions of all impact parameters. With the Plastic Ball/Wall spectrometer for the first time 4π data are available to investigate this subject.

For the investigation of entropy it is important to compare protons and clusters originating from the primordial interaction zone. Particles coming from the late state of the reaction or from the spectator regions are predominantly emitted with low energies[13]. An adequate way to eliminate those contributions is to apply a lower threshold for 40 MeV per nucleon to the data. There is also an upper energy limit due to the particle identification scheme of the Plastic Ball where, e.g., the punch-through deuterons above ~400 MeV are treated as protons. Furthermore, this study is limited to data at emission angles of 9° $\leq \theta \leq$ 160° ignoring the small yield of mainly spectator particles going into 0° to 9°. Fig. 4a,b shows the mean ratio of d/p and d-like/p-like as a function of charged particle multiplicity for 400 MeV/u ^{40}Ca + Ca. Figure 4c,d shows these ratios in each event as a contour plot. Each plot contains approximately 140 000 events. These cutoffs and limits mentioned above should be incorporated into comparisons with theoretical models since values obtained this way for ratios of d_{like}/p_{like} are lower than those extracted from the full spectrum. For symmetric systems these limits in particle identification can be overcome for extracting mean values by integrating in the center of mass only the back hemisphere where full particle identification is achieved. Ratios of yields $\tilde{d}$-like/$\tilde{p}$-like extracted in this way are referred to as "backward hemisphere values" and should be used for comparison with theoretical models, where no experimental bias simulation is easily possible. Those data are used in the following discussion on the median size of cluster production.

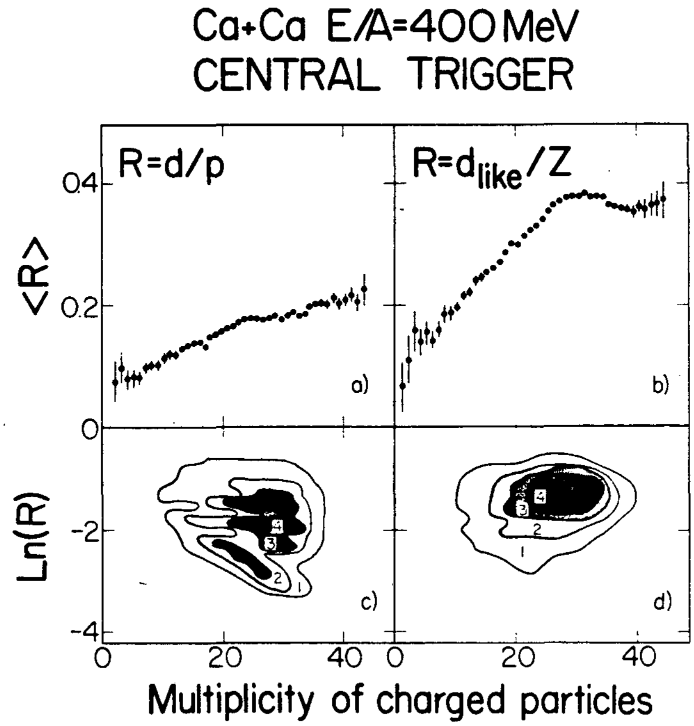

Fig. 4

The increase in deuteron production with increasing multiplicity can be described by the coalescence model[14] but improved by Sato and Yazaki[15]. It takes now into account both the size of the deuteron and the volume of the participant region. The coalescence radius p_0 in momentum space is related to the deuteron radius r_d and that of the participant volume r_p via

$\frac{\text{d-like}}{\text{p-like}^2} = \frac{4\pi}{3} p_o^3 \approx \frac{1}{(r_d^2 + 2r_p^2)^{3/2}}$, while r_p can be related to the observed charges by $r_p = r_0(2\ \text{p-like})^{1/3}$ with r_0 as a free parameter. Figure 5a shows a fit to the backward hemisphere Ca + Ca data with $r_d/r_0 = 2.9$ for 400 MeV/u and $r_d/r_0 = 1.9$ for 1050 MeV/u.

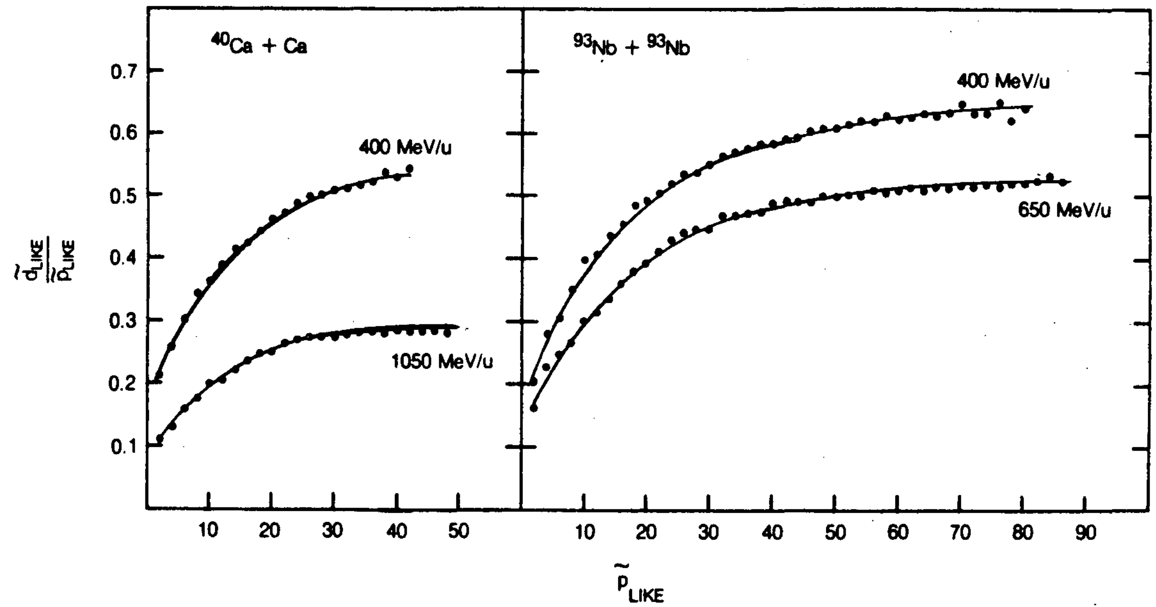

Fig. 5

The analysis of the 400 MeV/u and 650 MeV/u Nb data shows in fig. 5b approximately the same cluster production as in 400 MeV/u Ca + Ca when only events with the same number of participants were compared and not the average reaction. The average reaction in both cases is very different because of the larger average numbers of participants in Nb + Nb. Furthermore, a comparison of the cluster production at different bombarding energies but fixed number of participants yields a decrease with increasing energy. Up to now conclusions on entropy production in relativistic nuclear collisions were based only on single particle inclusive data and turned out to be quite puzzling[16]. Looking at these new 4π data several of these puzzling effects can now be understood:

i) The observed mass dependence in "S/N" goes along with a different average multiplicity, i.e., different size of the finite systems and therefore different cluster production.

ii) The weak increase in entropy with beam energy[16] is due to the comparison of d/p at different average multiplicities for different energies.

iii) The large entropy values at the average multiplicity must be replaced by the asymptotic ones, which are much closer to the calculated ones[10,11], and the introduction of new degrees of freedom as suggested in ref. 11 seems not necessary at this point.

This work was supported in part by the Director, Office of Energy Research, Division of Nuclear Physics of the Office of High Energy and Nuclear Physics of the U.S. Department of Energy under Contract DE-AC03-76SF00098.

References

1) A. Baden, H.H. Gutbrod, H. Löhner, M.R. Maier, A.M. Poskanzer, T. Renner, H. Riedesel, H.G. Ritter, H. Spieler, A. Warwick, F. Weik, H. Wieman, Nucl. Instr. Meth. 203, 189 (1982)
2) G.D. Westfall, J. Gosset, P.J. Johansen, A.M. Poskanzer, W.G. Meyer, H.H. Gutbrod, A. Sandoval, R. Stock, Phys. Rev. Lett. 37, 1202 (1976)
3) J. Gosset, H.H. Gutbrod, W.G. Meyer, A.M. Poskanzer, A. Sandoval, R. Stock, G.D. Westfall, Phys. Rev. C16, 629 (1977)
4) A. Mekjian, Phys. Rev. Lett. 38, 640 (1977), Phys. Rev. C17, 1051 (1978)
5) A. Sandoval, H.H. Gutbrod, W.G. Meyer, R. Stock, Ch. Lukner, A.M. Poskanzer, J. Gosset, J.C. Jourdain, C.H. King, G. King, Nguyen Van Sen, G.D. Westfall, K.L. Wolf, Phys. Rev. C21, 1321 (1980)
6) R. Stock, LBL-12652, May 1981
7) Y. Yariv and Z. Fraenkel, Phys. Rev. C20, 2227 (1979), Phys. Rev. C24, 488 (1981)
8) H.H. Gutbrod, H. Löhner, A.M. Poskanzer, T. Renner, H. Riedesel, H.G. Ritter, A. Warwick, F. Weik, and H. Wieman, submitted to Phys. Lett.
9) E.A. Remler, Ann. Phys. (N.Y.) 136, 293 (1981)
10) H. Stöcker, W. Greiner, and W. Scheid, Z. Physik A286, 121 (1978); H. Stöcker, J. Maruhn, and W. Greiner, Phys. Lett. 81B, 303 (1979)
11) P. Siemens and J. Kapusta, Phys. Rev. Lett. 43, 1486 (1979)
12) G. Bertsch and J. Cugnon, Phys. Rev. C24, 2514 (1981); J. Cugnon, Nucl. Phys. A387, 191c (1982)
13) H.H. Gutbrod, A.I. Warwick, and H. Wieman, Nucl. Phys. A387, 177c (1982)
14) H.H. Gutbrod, A. Sandoval, P.J. Johansen, A.M. Poskanzer, J. Gosset, W.G. Meyer, G.D. Westfall, R. Stock, Phys. Rev. Lett. 37, 667 (1976)
15) H. Sato and K. Yazaki, Phys. Lett. 98B, 153 (1981)
16) S. Nagamiya, M.C. Lemaire, E. Moeller, S. Schnetzer, G. Shapiro, H. Steiner, and I. Tanihata, Phys. Rev. C24, 971 (1981)

Global Analysis of Relativistic Nuclear Collisions Detected by the Plastic Ball

H.G. Ritter, H.A. Gustafsson, H.H. Gutbrod, B. Kolb, H. Löhner,
B. Ludewigt, A.M. Poskanzer, T. Renner, H. Riedesel, A. Warwick,
F. Weik, and H. Wieman

Gesellschaft für Schwerionenforschung, Planckstrasse 1
D-6300 Darmstadt 11, West Germany
and
Nuclear Science Division, Lawrence Berkeley Laboratory
University of California, Berkeley, CA 94720

Data from 4π detectors like the Plastic Ball are ideally suited to study the event shapes and emission patterns of high energy nuclear collisions. It has been pointed out that event shape analysis might be able to distinguish between predictions of cascade and hydrodynamical models. To do this the thrust [1-3] and sphericity [2,4] analyses used in high energy physics [5] have been proposed. Because the thrust vector cannot be calculated analytically, the sphericity method generally has been used.

The sphericity tensor

$$F_{ij} = \sum_{\nu} p_i(\nu)\; p_j(\nu)\; w(\nu)$$

is calculated from the momenta of all measured particles for each event. It is appropriate to choose the weight factor w(ν) in a way that composite particles have the same weight as the individual nucleons of the composite particle at the same velocity. In this paper the weight $w(\nu) = 1/(2m)$ as proposed in ref. 4 (kinetic energy flow) is used. Other coalescense invariant weights such as 1/p [2] have been proposed and have been used in our analysis. The sphericity tensor approximates the event shape by an ellipsoid whose orientation in space and aspect ratios can be calculated by diagonalizing the tensor.

The shapes predicted by hydrodynamical and cascade calculations are quite different. The hydrodynamical model predicts prolate shapes along the beam axis for grazing collisions. With decreasing impact parameter the flow angle increases up to 90 degrees for zero impact parameter events and the shape becomes prolate [1,3,4]. This behavior is independent of projectile and target mass. Cascade calculations, on the other hand, predict finite nontrivial flow angles only for very heavy systems [4].

A rigorous comparison of experimental data with predictions is only possible if the theory calculates all observed quantities by generating a large number of complete events. Those events have to be filtered with the known experimental acceptance and efficiency of the detector. Most models, however, have not yet reached sufficient sophistication: cascade models do not include composite particles, and hydrodynamical codes do not yet produce event-by-event fluctuations. This makes a useful comparison difficult, and it is not yet clear that the differences between the two models will show up after all distortions are taken into account.

Another big obstacle in extracting information from a flow analysis is fluctuations due to finite particle effects. Recently, Danielewicz and Gyulassy [6] have shown that those distortions strongly depend on multiplicity and that the flow angle, θ, if properly weighted by the Jacobian (sinθ), is much less severely shifted towards higher values than the aspect ratios. It now can be shown that the results of the flow analysis of the

400 MeV/u Ca + Ca data [7], even though they differ from cascade predictions, can be explained with finite number distortions by assuming prolate shapes along the beam axis [8]. Deviations from cascade predictions seen in the analysis of asymmetric target projectile combinations measured with the streamer chamber [9,10] seem to be inconclusive as well because the data points in the flow plot do not fall in the region where, despite the distortions, nontrivial flow angles and aspect ratios can be detected.

It is hoped that heavier symmetric systems are less sensitive to distortions and that possible macroscopic effects can more easily be detected. As shown in fig. 1, the Nb + Nb data at 400 MeV/u reach flow angles up to 30 degrees (peak maximum) for the highest multiplicity bins, whereas predictions from the Yariv-Fraenkel cascade [11], filtered with the exact acceptance and efficiency of the Plastic Ball [12] never deviate significantly from 0 degrees even for the highest multiplicity events. The fact that finite flow angles are seen in the data indicates that in those events there exists a plane defined by the flow axis and the beam axis, which will be called the reaction plane. All events can be rotated by the azimuthal angle φ determined by the flow analysis so that their individual reaction planes all fall into the x-z plane, with the z-axis being the beam axis. For those rotated events rapidity plots in the reaction plane [3,13] can be calculated. The use of $p_\perp/m$ as proposed in ref. 3 is only of theoretical interest as the phase space vanishes. However, the invariant cross sections dp_x/mdy (in plane) and dp_y/mdy (out of plane) can be plotted, where p_x is the projection of the perpendicular momentum into the reaction plane and p_y the projection into the plane perpendicular to the reaction plane. Figure 2 shows these plots for 400 MeV/u Nb + Nb data and cascade calculations for events with charged particle multiplicities between 40 and 50. The depletion near target rapidities is due to experimental acceptance. The two cascade plots and the out-of-plane data plots are symmetric around the beam axis, whereas the in-plane data plot is clearly asymmetric with the highest intensity contour, resulting largely from the projectile remnants, indicating a definite deflection. The multiplicity dependence of the outer contour lines seems to follow the trend indicated by the flow angle distributions (fig. 1). However, the position of the peak from the projectile remnants changes only slightly with multiplicity and corresponds at its maximal sidewards position to a momentum transfer of about 50 MeV/c per nucleon. The comparison of the experiment with hydrodynamical calculation [3] is not straightforward as the impact parameter can be related to multiplicity only via cascade calculations. The hydrodynamical prediction for the flow angle seems to be qualitatively in agreement with the measurement, but the very small variation of the deflection of the projectile as a function of multiplicity does not show the behavior predicted by hydrodynamics.

For asymmetric systems the flow analysis is usually performed in the center of mass of all the measured particles. The velocity β_{obs} of this system in the beam direction should depend on the impact parameter and thus on the multiplicity of charged particles m_c. Figure 3 shows a contour plot of m_c as a function of the calculated velocity β_{obs} for the reaction 800 MeV/u Ne + Pb. The observed velocity varies from that of the nucleon-nucleon system β_{NN} for the most peripheral collisions up to the velocity of the compound system β_{comp}. It significantly overshoots the fireball system velocity β_{FB} even though only about one-third of all particles (and preferentially the faster ones) are detected. This strongly indicates not only that the projectile is stopped as, e.g., predicted by a clean-cut fireball model [14] but that the target nucleus as a whole stops the projectile. The emission pattern of this "compound" system can be studied by a flow analysis. The flow angle distributions $dN/d\cos\theta$ for the different multiplicities all peak at 0 degrees, but for the highest multiplicities they become flat and angle independent, indicating isotropic emission. The same pattern is suggested by the rapidity plots.

From the analysis of the presently available Plastic Ball data, one can conclude that no indication for flow is seen in the symmetric mass 40 system. For the Nb data the flow angle distribution seems to be in agreement with hydrodynamical predictions, whereas the in-plane rapidity plots show an ambiguous result. The pattern found in the asymmetric system investigated so far is compatible with sperical emission at the highest multiplicities. It will be interesting to study the energy and mass dependence of these effects.

This work was supported in part by the Director, Office of Energy Research, Division of Nuclear Physics of the Office of High Energy and Nuclear Physics of the U.S. Department of Energy under Contract DE-AC03-76SF00098.

References

1. J. Kapusta and D. Strottman, Phys. Lett. 103B (1981) 269
2. J. Cugnon, J. Knoll, C. Riedel, and Y. Yariv, Phys. Lett. 109B (1982) 167
3. H. Stöcker, L.P. Csernai, G. Graebner, G. Buchwald, H. Kruse, R.Y. Cusson, J.A. Maruhn, and W. Greiner, Phys. Rev. C25 (1982) 1873
4. M. Gyulassy, K.A. Fraenkel, and H. Stöcker, Phys. Lett. 110B (1982) 185
5. S. Brandt and H. Dahmen, Z. Physik C1 (1979) 61
   S.L. Wu and G. Zoberning, Z. Physik C2 (1979) 107
6. P. Danielewicz and M. Gyulassy, Lawrence Berkeley Laboratory Preprint 15721, submitted to Physics Letters B
7. H.G. Ritter, in Proc. 3rd Intl. Conf. on Nuclear Reaction Mechanism, ed. E. Gadioli (Varenna, Italy, 1982)
   H.H. Gutbrod, H. Löhner, A.M. Poskanzer, T. Renner, H. Riedesel, H.G. Ritter, A. Warwick, F. Weik, and H. Wieman, in Proc. Intl. Conf. on Nucleus-Nucleus Collisons (Michigan State University, East Lansing, MI, 1982), Lawrence Berkeley Laboratory Preprint 14980
8. P. Danielewicz, private communication, 1983
9. H. Stroebele, R. Brockmann, J.W. Harris, F. Riess, A. Sandoval, H.G. Pugh, L.S. Schroeder, R.E. Renfordt, T. Tittel, and M. Maier, Phys. Rev. C27 (1983) 1349
10. A. Hufe, D. Beavis, S.Y. Fung, W. Gorn, D. Keane, J.J. Lu, R.T. Poe, B.C. Shen, and G. VanDalen, Phys. Rev. C27 (1983) 439
11. Y. Yariv and Z. Fraenkel, Phys. Rev. C20 (1979) 2227
12. A. Baden, H.H. Gutbrod, H. Löhner, M.R. Maier, A.M. Poskanzer, T. Renner, H. Riedesel, H.G. Ritter, H. Spieler, A. Warwick, F. Weik, and H. Wieman, Nucl. Instr. and Meth. 203 (1982) 189
13. H. Stöcker, G. Buchwald, G. Graebner, J. Maruhn, W. Greiner, K. Fraenkel, and M. Gyulassy, Michigan State University Preprint MSUCL 409
14. J. Gosset, H.H. Gutbrod, W.G. Meyer, A.M. Poskanzer, A. Sandoval, R. Stock, and G.D. Westfall, Phys. Rev. C16 (1977) 629

Figure Captions

Fig. 1: Frequency distributions of the flow angle θ for different multiplicity bins (data and cascade calculations).

Fig. 2: Contour plots (linear contours) of the projection of the transverse momentum in and out of plane as a function of cm rapidity.

Fig. 3: Contour plot (linear contours) of the charged particle multiplicity as a function of the velocity of the cm system of the measured charged particles.

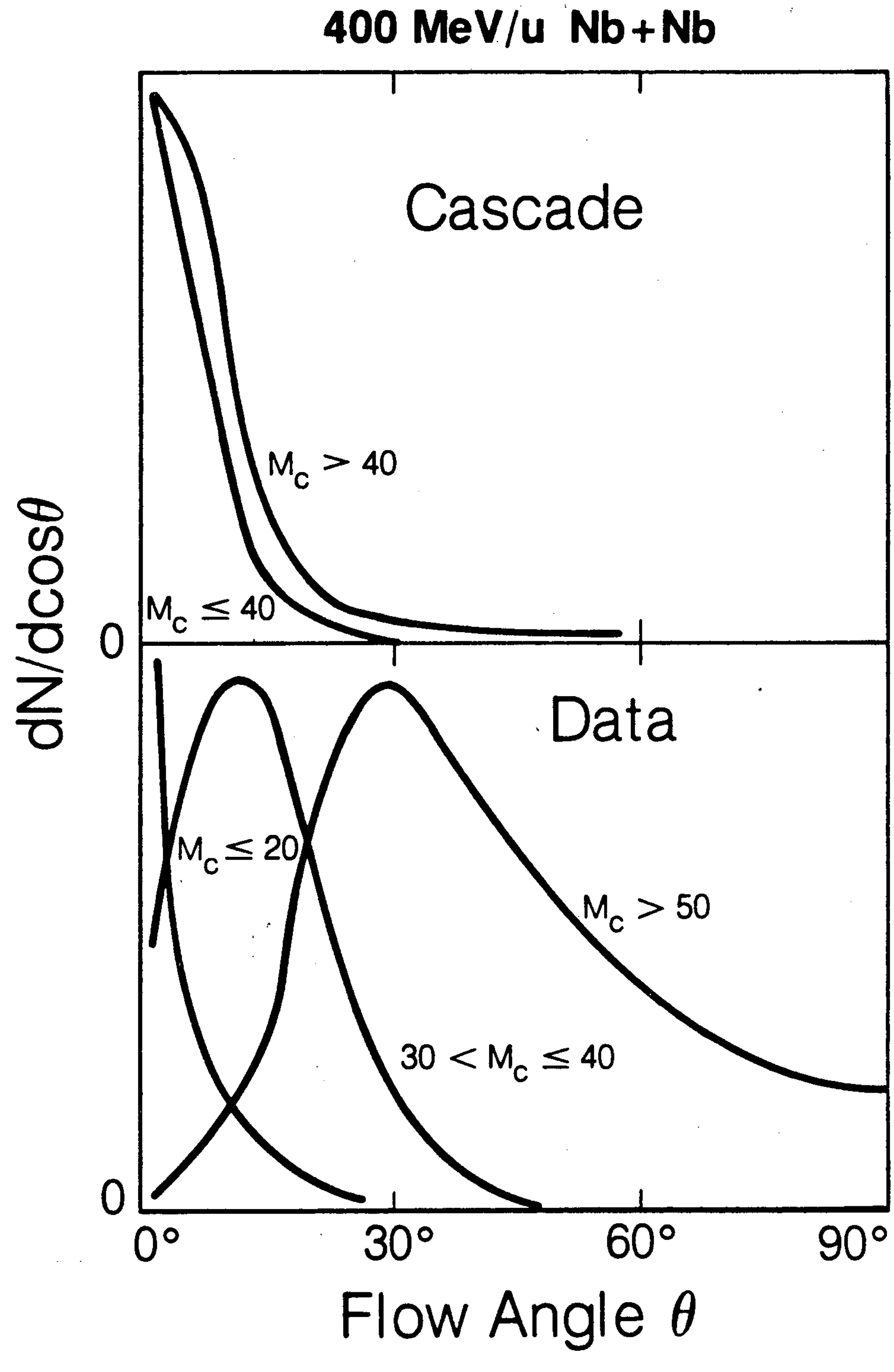
400 MeV/u Nb+Nb
Cascade
$M_c > 40$
$M_c \leq 40$
Data
$M_c \leq 20$
$M_c > 50$
$30 < M_c \leq 40$
dN/dcosθ
0
0
0°
30°
60°
90°
Flow Angle θ

Fig. 1

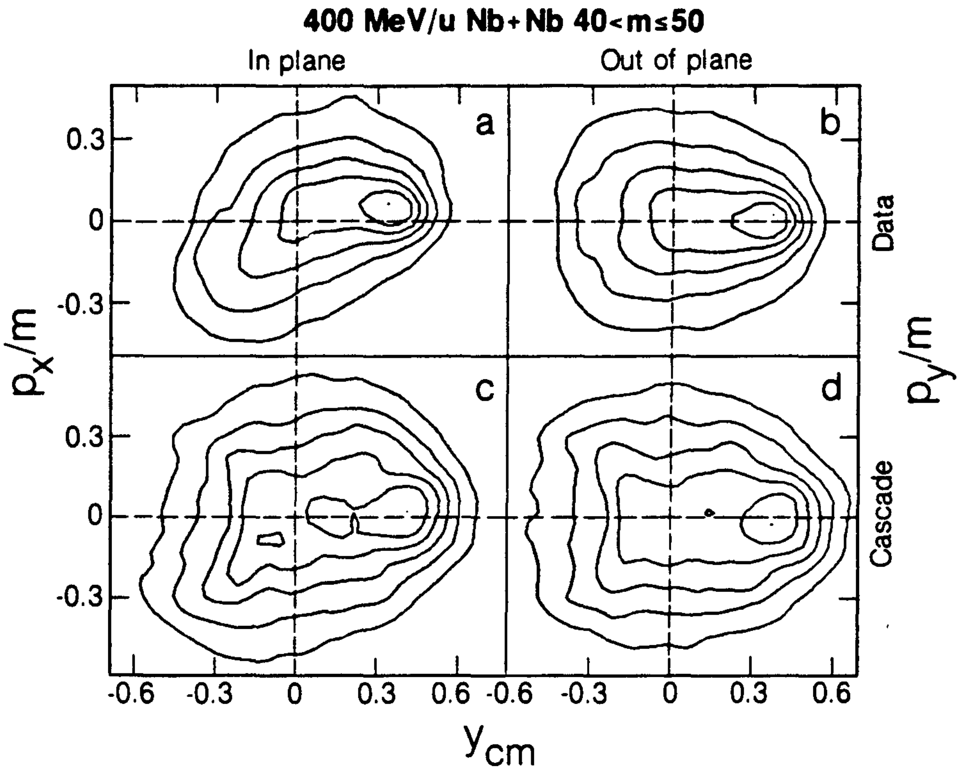
400 MeV/u Nb+Nb 40<m≤50
In plane
Out of plane
a
b
c
d
Data
Cascade
0.3
0
-0.3
p_x/m
p_y/m
-0.6 -0.3 0 0.3 0.6 -0.6 -0.3 0 0.3 0.6
y_{cm}

Fig. 2

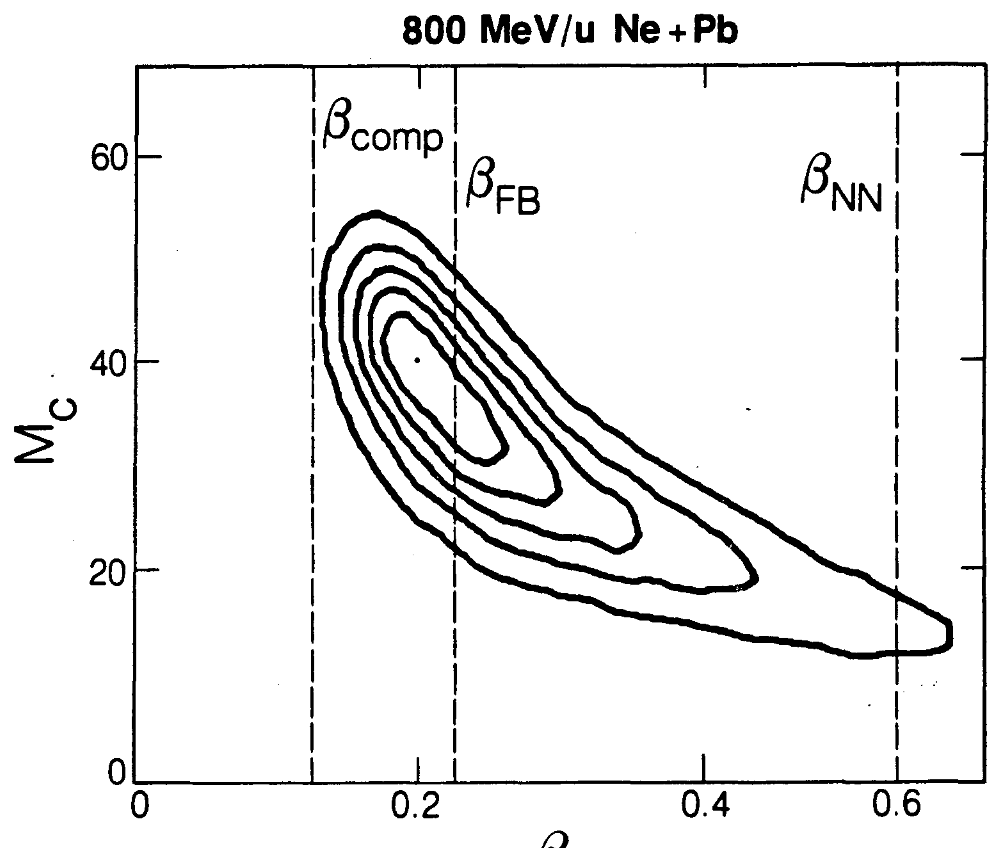
800 MeV/u Ne+Pb
β_{comp}
β_{FB}
β_{NN}
60
40
20
0
M_C
0
0.2
0.4
0.6
β

Fig. 3

Two Particle Correlations Observed with the Plastic Ball Detector

H. Wieman, H.H. Gutbrod, H.A. Gustafsson, B. Kolb,
H. Löhner, B. Ludewigt, A.M. Poskanzer, T. Renner,
H. Riedesel, H.G. Ritter, A. Warwick, and F. Weik

Gesellschaft für Schwerionenforschung, Planckstrasse 1
D-6300 Darmstadt 11, West Germany and
Nuclear Science Division, Lawrence Berkeley Laboratory
University of California, Berkeley, CA 94720, USA

Three different categories of two-particle correlations are being investigated in the analysis of the Plastic Ball data. The first category, which has already received the most attention by others in the field of relativistic heavy ions, is source size determination using Hanbury-Brown, Twiss type interferometry. Two-pion correlations have been measured for this purpose with a streamer chamber[1] and with a magnetic spectrometer.[2] Source size measurements have also been made with proton-proton correlations[3] following the calculations of Koonin,[4] which include Coulomb and nuclear forces in addition to strictly interference effects. In this category of two-particle correlations the relative velocities are quite low. For protons the kinetic energy in the center of mass of the pair is on the order of 0.5 MeV.

The second category of two-particle correlations deals with low-energy nuclear cluster formation, the kinetic energy in the pair center of mass being in the region 1 MeV to 10 MeV. Here one observes nuclear composites--the formation and decay of particle unstable isotopes and levels such as ^{5}Li.

The third category addresses higher energies, 100 MeV or more in the center of mass of the pair. In this energy region the possibility exists for seeing baryon resonances. For example, delta decay might be observed via π^+-p correlations or dibaryon resonances by π^+-d correlations.[5]

Here we shall be reporting only on preliminary results obtained in the first two categories. So far, source sizes and cross sections have not been extracted as we have mainly been exploring, looking for those areas where the unique features of the Plastic Ball can best be exploited. The most obvious advantage of the Plastic Ball for two-particle correlation measurements is the large solid angle ($\sim 4\pi$) and rapid data collection, which allow better statistics than are easily obtained with other devices. On the other hand, the relatively coarse angular resolution (3.5° to 10°) and the limited energy resolution impose restrictions on the correlations that can be measured. The studies described here have been limited to the possible two-particle combinations of p, d, t, ^{3}He, and ^{4}He with low relative velocities. Particles included in the analysis were stopped in the Ball detector (laboratory angle 10° to 160°) where particle type and energy could be determined. As work progresses the correlations will be compared for various projectile target combinations, but to date our efforts have been concentrated on Ca + Ca at E/A = 400 MeV, the system for which we have the largest data set. These data were recorded using a central collision trigger.

The correlation function $F(\Delta p)$ has been generated in a manner similar to that used in two-particle interferometry studies.[3]

$$F(\Delta p) = nN_s(\Delta p)/N_d(\Delta p)$$

where $N_s(\Delta p)$ is the number of pairs per unit Δp taken from the same event and $N_d(\Delta p)$ are the number of pairs per unit Δp constructed from different events. The momentum Δp is the particle momentum in the center of mass of the pair. The factor n is chosen arbitrarily such that $F(\Delta p)$ equals approximately one at large Δp. This correlation function is closely related to the R correlation function used by Koonin: $F(\Delta p) - 1 \cong R(\Delta p)$. $F(\Delta p)$ is greater than 1 for positive correlations. The particle momentum in the center of mass (Δp) was chosen for this analysis for two reasons. First, this choice is consistent with the variable used in other source size determinations ($\Delta p \cong |\vec{p}_1 - \vec{p}_2|/2$ for pairs of like massed particles). Second, Δp is easily related (nonrelativistically) to Q values and excitation energies (E_x) of clusters formed from the pair, i.e.,

$$\Delta p = \sqrt{2 \frac{m_1 m_2}{m_1 + m_2} (E_x + Q)} \quad .$$

The resulting correlation function for proton-proton pairs is shown in fig. 1. The two solid curves shown with the measured correlation function are predictions[4] for Gaussian sources with rms radii of $r_0 = 3$ fm and 5 fm and a lifetime of $\tau = 0$. The expected enhancement in the measured correlation function is clearly observed, but it peaks at 30 MeV/c instead of 20 MeV/c, Koonin's predicted value. Also the peak is broader than predicted. Both of these distortions can be blamed on the finite angle subtended by a Plastic Ball detector module. This distortion, however, is probably not a serious problem for a source size analysis, since the integrated peak area should be as sensitive as the peak height to the source radius.

We have found that p-p is not the only two-particle system to show correlations at low Δp. A number of other two-particle systems exhibit stronger correlations, some positive, some negative. The most striking examples appear in figs. 2 and 3. As shown, there is a strong enhancement in the p-^{4}He system at a Δp value corresponding to the decay of the ^{5}Li ground state. Likewise, d-^{4}He has a peak that apparently comes from the decay of the lowest excited levels of ^{6}Li. For the d-d system, on the other hand, there is a negative correlation. At low relative velocity deuterons appear to coalesce into excited states of ^{4}He that decay by another channel. The observed depression in the d-d correlation function extends up to $\Delta p = 150$ MeV/c. This is well beyond the $\Delta p = 55$ MeV/c instrumental cutoff imposed by the finite angular size of the detectors in the Plastic Ball. The d-d system may be contrasted with the p-t system, which couples to slightly lower values of ^{4}He excitation. In this case there is evidence again of a positive correlation at low Δp. A summary of observed correlations is shown in table 1 along with the Q value for the various pairings of the particles. The Q value seems to be important for lithium and beryllium; positive correlations are only observed when the pairs couple to the ground state or lowest excited states of the composite.

Let's now consider another aspect of two-particle correlations that we have investigated, the effect of particle multiplicity. Some measured correlation functions are shown in figs. 4 and 5 with two different cuts on particle multiplicity. The selection of high and low multiplicity events correspond to the tails on either side of the particle multiplicity distribution. For proton-proton correlations the multiplicity dependence of the enhancement at low Δp (fig. 4) is quite striking. The peak height is roughly six times larger for low multiplicity events compared to high multiplicity events. Likewise, there is significant multiplicity dependence in the p-^{4}He correlation function (fig. 5), a factor of three difference between high and low multiplicity. If we interpret the multiplicity dependence of the p-p correlations in light of Koonin's predictions it is clear that there is a strong dependence of source size on particle multiplicity. This effect will be pursued more quantitatively in the future.

The results obtained so far show that the Plastic Ball with its large solid angle can be a useful tool for measuring two-particle correlations. The present effort on two-particle correlations will continue along two lines. First, work will continue towards extracting source size information from proton-proton correlations. The initial question is how much does the limited detector angular resolution distort the true correlation function, and is this important? Perhaps the integrated peak in the correlation function is sufficient for source size measurements. There is the additional, more fundamental question, what is the meaning of the source size? Maybe this is the freeze-out radius since correlations from an earlier stage would probably be largely destroyed through later interactions.

The second line of effort will be devoted to extracting relative cross sections for the formation of the particle-unstable isotopes and levels that we have observed. These can then be compared with phase space models such as Fai and Randrup's,[6] which predict yields of stable as well as unstable clusters.

This work was supported in part by the Director, Office of Energy Research, Division of Nuclear Physics of the Office of High Energy and Nuclear Physics of the U.S. Department of Energy under Contract DE-AC03-76SF00098.

References

1. J.J. Lu, et al., Phys. Rev. Lett. 46, 898 (1981)
2. J.A. Bistirlich, et al., LBL-13366, 146 (1982)
3. F. Zarbakhsh, et al., Phys. Rev. Lett. 46, 1268 (1981)
4. S.E. Koonin, Phys. Lett. 70B, 43 (1977)
5. T. Siemiarczuk, J. Stepaniak, private communication, 1983
6. J. Randrup, G. Fai, Phys. Lett. 115B, 281 (1982)

Figure Captions

Fig. 1. p-p two-particle correlation function as a function of the particle momentum in the center of mass of the pair. Solid curves are predictions of Koonin for sources with rms radii of $r_0 = 3$ fm and 5 fm. The source lifetime is $\tau = 0$. Values of $F(\Delta p)$ greater than 1 indicate a positive correlation.

Fig. 2. Two-particle correlation functions for d-^{4}He coupling to ^{6}Li and p-^{4}He coupling to ^{5}Li. Position of levels known to decay to the pair particles are indicated.

Fig. 3. Two-particle correlation functions for d-d p-t both coupling to ^{4}He. Correlations are shown as a function of the particle momentum in the center of mass of the pair. Position of some ^{4}He excited states are indicated in the p-t system.

Fig. 4. p-p two-particle correlation function as in fig. 1 but event selected for high and low particle multiplicity.

Fig. 5. p-^{4}He two-particle correlation function as in fig. 2 but event selected for high and low particle multiplicity.

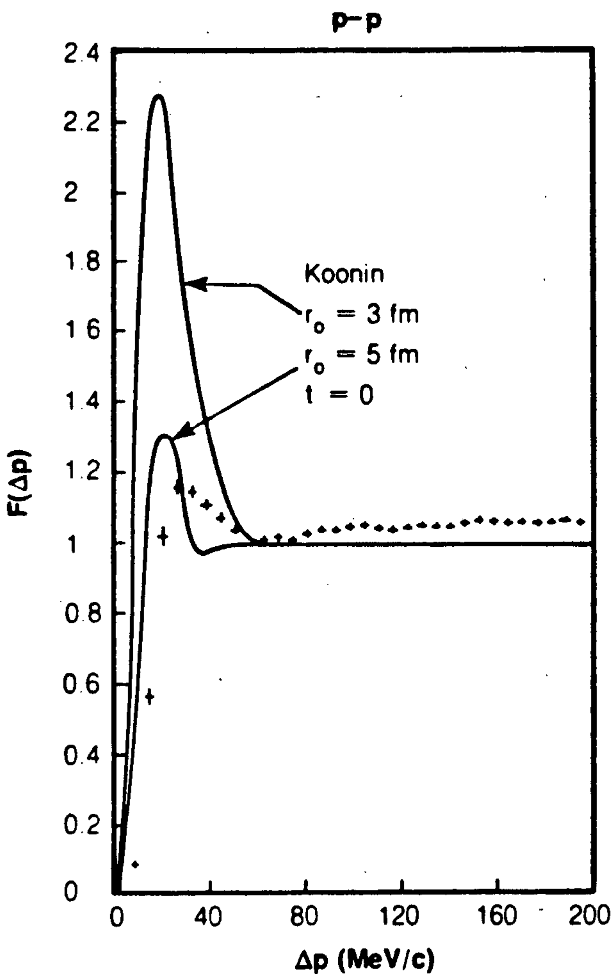
p-p
F(Δp)
2.4
2.2
2
1.8
1.6
1.4
1.2
1
0.8
0.6
0.4
0.2
0
Koonin
r_o = 3 fm
r_o = 5 fm
t = 0
0
40
80
120
160
200
Δp (MeV/c)

Fig. 1

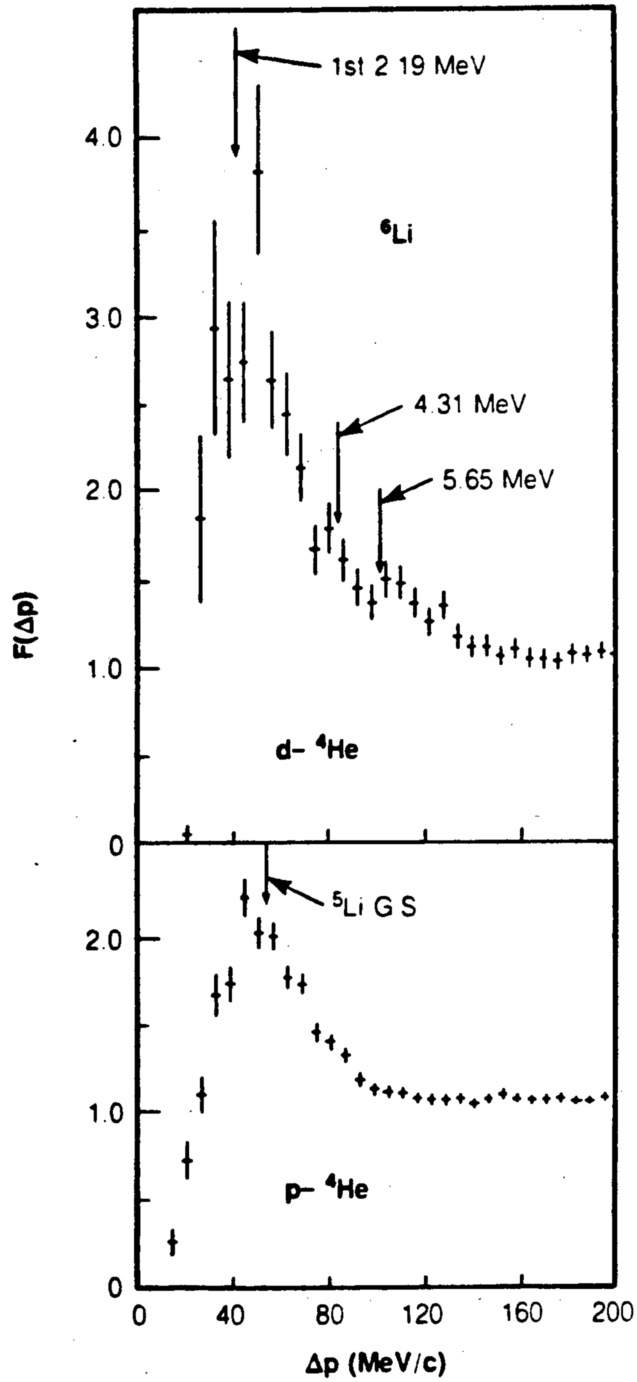
1st 2.19 MeV
4.0
3.0
2.0
1.0
0
⁶Li
4.31 MeV
5.65 MeV
F(Δp)
d- ⁴He
⁵Li G.S.
2.0
1.0
0
p- ⁴He
0
40
80
120
160
200
Δp (MeV/c)

Fig. 2

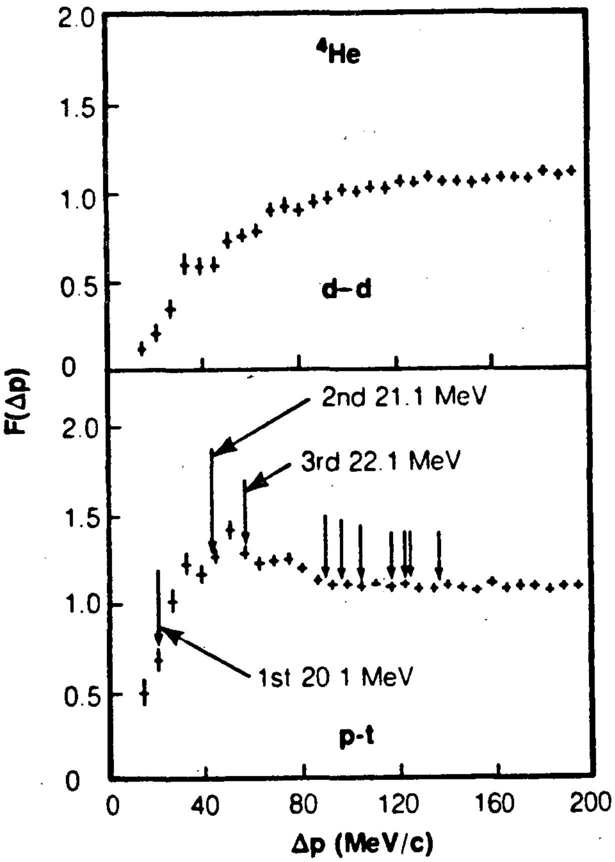

Fig. 3

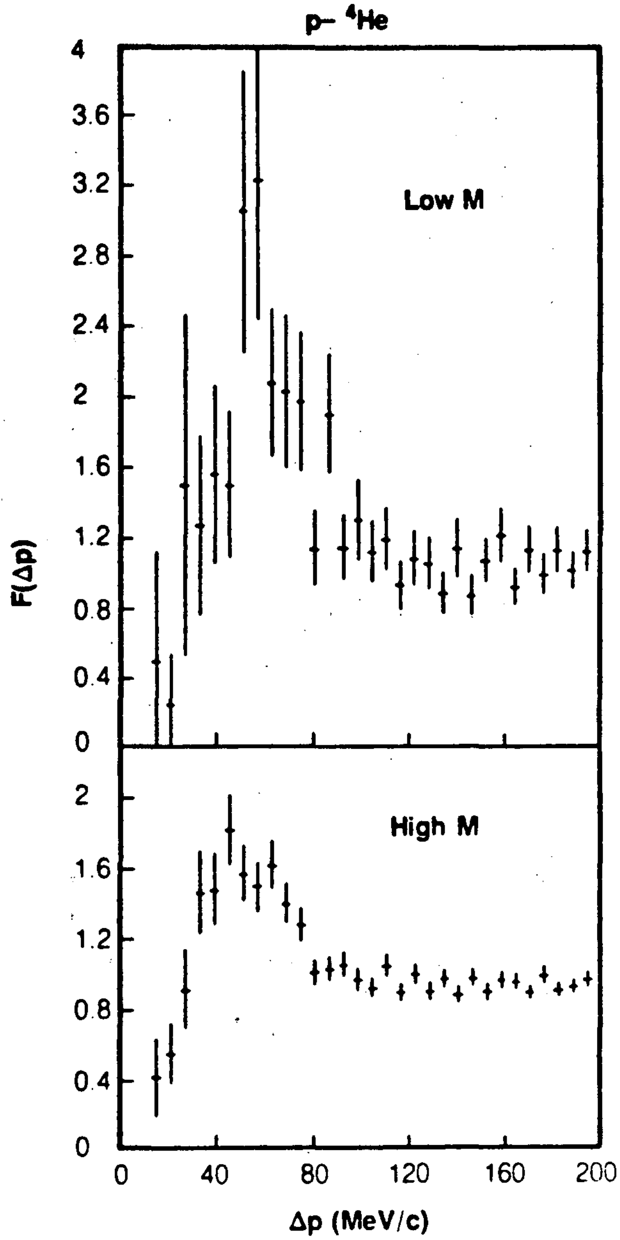

Fig. 5

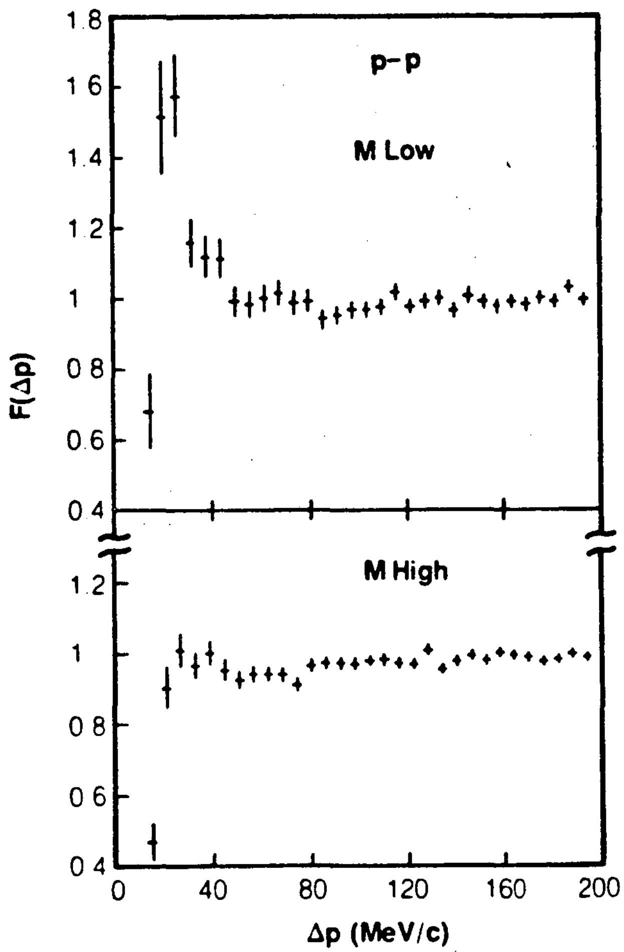

Fig. 4

Table 1

Two-Particle Correlations

Low Δp

	p	d	t	^{3}He	^{4}He
^{4}He					^{8}Be Q = -0.09 corr. pos.
^{3}He				^{6}Be Q = 11.5 --	^{7}Be Q = 1.6 corr. pos.
t			^{6}He Q = 12.3 corr.∿pos.	^{6}Li Q = 15.8 corr. --	^{7}Li Q = 2.5 corr. pos.
d		^{4}He Q = 23.8 corr. neg.	^{5}He Q = 16.7 corr. --	^{5}Li Q = 16.4 corr. --	^{6}Li Q = 1.47 corr. pos.
p	^{2}He -- corr. pos.	^{3}He Q = 5.5 corr. neg.	^{4}He Q = 19.8 corr. pos.	^{4}Li Q = -2.9 corr. pos.	^{5}Li Q = -2.0 corr. pos.